Iraqi Journal of Industrial Research (IJOIR)

Journal homepage: http://ijoir.gov.iq

Biosynthesis of Silver Nanoparticles from *Microbacterium sp*. for Determination of Antibacterial and Antitumor

[1]Thuraya Mehbas Dewan*, [2]Rashid Rahim Hateet

[1]Quality Control Department, Misan Mill, State Company for Petrochemical Industries, Ministry of Industry and Minerals – Iraq

[2]Department of Biology, College of Science, University of Misan – Iraq

Article information

Article history:
Received: January, 07, 2023
Accepted: May, 28, 2023
Available online: October, 20, 2023

Keywords:
Silver Nanoparticles,
Antibacterial,
Antitumor

Corresponding Author:
Thuraya Mehbas Dewan
thurayadewan@gmail.com

DOI:
https://doi.org/10.53523/ijoirVol10I2ID305

Abstract

Synthesizing of AgNPs with a cost effective, environmentally friendly in simple ways, then use them as antibacterial and as anticancer on breast cancer cell line. The soil samples were collected from different places. Isolated, then purified, identified genotypically by *16Sr RNA* sequencing analysis and compared with NCBI, GenBank which identified as *Microbacterium* sp., and there was a new strain discovered for the first time in Iraq register in our name and gave a new sequence ID in GenBank. Biosynthesis of AgNPs using extracellular synthesis by reducing Ag^{+} to Ag^{0} and forming silver nanoparticles. The color (reddish brown) was the first indicator of the formation of AgNPs, which was characterizing by using: UV-Visible Spectroscopy, XRD (X-ray diffraction), SEM (Scanning Electron Microscopy), EDX (Energy Dispersive Spectroscopy X-ray), AFM (Atomic Force Microscopy).Biological identification of AgNPs was determination by antimicrobial activity of biosynthesized AgNPs, the specimens collected from Al- Sadr hospital / Misan (identified by using VITEK 2). The result showed inhibition zone on pathogenic bacteria range (6- 38mm), and compared with Gentamycin antibiotic on same specimens. By the using of MTT test against breast cancer cells (MCF7 cell line), antitumor activity of were determined and showed very high results. The breast cancer cell line inhibition by about 81% at 100µg/ml, the rate of inhibition was very good and strongly suppressed MCF-7 cell lines proliferation, so different biomedical field can be used from AgNPs as antibacterial and anticancer agents, with considerable results.

1. Introduction

Nanotechnology is the transformation of single atoms, molecules, or compounds into structures to create materials that range in size from 1 to 100 nm with unique properties. They can be divided based on their features, forms, and sizes into many categories. Because of their large surface area and nanoscale size, the NPs have unique physical and chemical characteristics. A variety of applications by metal nanoparticles are widely

utilized in biotechnology and biomedicine field. Microorganisms' biosynthesized silver nanoparticles -AgNPs- The emergence of microbial illnesses has recently been considerably accelerated by human immunological compatibility. In order to protect people from various diseases, a variety of novel antibiotics and therapeutic pharmaceutical substances have been made available on the market [1]. However, they have the potential to have an adverse impact on the environment, particularly in developing countries. Although little is known about their antibacterial properties, metals containing nanoparticles may be employed to treat a variety of infections. The creation of nanoparticles has become a popular topic at the intersection of nanotechnology and biotechnology due to a growing need for ecologically friendly products [2]. Biogenic synthesis of metal nanoparticles has been demonstrated using a variety of species [3], including bacteria, fungi, algae, actinomycetes, plants, and more.

It has been documented that actinobacteria such *Rhodococcus sp*., *Streptomyces sp*., and *Nocardia sp.* can produce and describe silver and gold nanoparticles [4]. Since their antibacterial characteristics have long been known, metals including zinc, silver, titanium, and copper are frequently employed in modern medicine to treat microbial infection illnesses. One theory holds that free metal ion toxicity produced by nanoparticle surfaces may be crucial for preventing infections. AgNPs are well known for their catalytic, electrical, and optical properties [5]. To stop infections, a new generation of dressings containing antibacterial substances like silver was developed [6]. Recent research has shown that amphiphilic hyper branched macromolecules and silver nanoparticle hybrids have effective antibacterial surface coatings [7]. Silver nanoparticles are in high demand due to their broad use. Among noble metal nanomaterials, silver nanoparticles have drawn a lot of interest due to their appealing physico-chemical characteristics [8]. Due to their surface plasmon resonance and substantial effective scattering cross section, individual silver nanoparticles make excellent candidates for molecular labeling [9]. Although the bactericidal effect of silver ions on bacteria is well established, the exact mechanism is only partially understood. The thiol groups of crucial enzymes are thought to bind strongly with ionic silver, leaving them inactive. Studies reveal that bacteria lose the ability to copy their DNA when exposed to silver ions. Other studies have discovered signs of changes in the structure of cell membranes as well as the formation of small, electron-dense granules from sulfur and silver. One of the most popular cancer therapies is chemotherapy. The majority of anticancer chemicals are generated and manufactured by microorganisms, especially *Actinomycetes*, which also produce a significant amount of natural products with biological and bioactive qualities, as well as the synthesis of silver and sulfur into small, electron-dense granules.

One of the most popular cancer therapies is chemotherapy. There are many antitumor substances in nature, either as whole substances or as derivatives. Most of these substances are formed and produced by microorganisms, particularly *Actinomycetes*, which also produce a large number of natural products with a variety of biological and bioactive properties in addition to antitumor properties. Such DNA cleavage is brought on by inhibition of topoisomerase I or II. In some cases, the inhibition of critical enzymes affects tumor-induced angiogenesis as well as signal transmission processes like proteases, mitochondrial permeabilization, and cellular metabolism. Experimental Procedure was to separate and identify microbes from soil.

2. Materials and Methods

2.1. Soil Samples Collecting

In sterile plastic bags, soil samples were taken at a depth of 11 cm from sugar cane fields and gardens in Misan. To lessen the amount of bacteria in the soil other than *Actinomycetes*, the soil samples were dried in an oven at 60°C for three hours. *Actinomycetes*, which in this study were *Microbacterium sp*., produce spores before growing in media [13].

2.2. Isolation Media

Each sample was serially diluted. The samples were cultured for 5 days at 30ºC using the isolation medium SCN Agar (Starch-casein-nitrite agar), which contains 1 ml of cycloheximide (100ùg/ml) as an antifungal agent. One colony of the isolated bacteria was grown in pure culture on transfer medium made of YEG agar (Yeast Extract Glucose agar) [10].

3.2. *16S rRNA* Gene Sequencing of Isolated Bacteria

Using universal primers [21] as shown in Table (1) has been utilized in a number of techniques for identifying DNA sequence. Genomic DNA was extracted from isolates using a DNA kit (Presto'Mini g DNA Bacteria Kit,

Geneaid, Taiwan). The PCR reaction mixture, which had a final volume of 20 l, was made up of 2 l for each of the 27F and 1492R primers (10 picomole), 9 l of de-ionized water, and 7 l of the isolate's DNA. These ingredients were added to the Maxime TM PCR Premix i-Taq (Intronbio/Korea), 30 cycles of denaturation at 94°C for 1 min, annealing at 58°C for 30 sec, and extension at 72°C for 1 min were performed, with the final extension taking place at 72°C for 7 min. On Agarose Gels the product that amplified was then Electrophoresis [11], then compared the isolation strain with (NCBI) GenBank to identify genotypically by *16S rRNA* sequencing analysis [12].

Table (1). Primer kite that use in this experiment of DNA extraction.

Primer	Sequence (5´- 3´)	Length	Amplicon size
27F	´AGAGTTTGATCCTGGCTCAG	20 bp	1500 bp
1492R	GGTTACCTTGTTACGACTT	19 bp	

2.4. Biosynthesis of AgNPs Laboratory

Colonies are transferred into conical flasks with 200 ml of MGYP (Malt extract glucose yeast extract peptone broth)7 at PH 7.0 and are then incubated for 7 days at room temperature in a shaker incubator (150 rpm). Colony then formed on the medium and was filtered via Whatman No. 1 filter paper (Sigma/USA).

Then added the supernatant to 2mM of $AgNO_3$ (1:1) the same volume of each one and cultured for 7 days at room temperature in an orbital shaker (150 rpm), the supernatant's color changed to a dark shade of reddish brown, signifying that AgNPs had formed in the culture medium [13], then characterized of the AgNPs by physical test at BPC-Analysis Center in Baghdad.

2.5. Characterization of Biosynthesis AgNPs [14]

2.5.1. UV-Visible Spectroscopy

In order to determine the absorption spectrum, silver nanoparticles that had been bio-synthesised in a lab setting were examined using UV-Vis spectroscopy (Elettrofor/Italy). The sample of bio-AgNPs was gathered in a quartz cuvette with a 1 cm path length and 2 ml of solution to fill past the instrument light path. While treated supernatants were being utilized to track their UV-Visible absorbance Spectra between 300 and 800 nm wave length, the untreated supernatant was employed as a reference control [15].

2.5.2. X-Ray Diffraction (XRD) Analysis

One of the most popular methods for characterizing NPs is X-ray diffraction (Broker/Germany). Crystal structure, phase nature, lattice parameters, and crystal sizes are typically revealed by XRD [16].

2.5.3 Transmission Electron Microscopy (TEM)

Transmission electron microscopy analysis (Broker/Germany), using magnified TEM micrographs, was used to determine the formation type (shape) and size of the created silver nanoparticles [17].

2.5.4 Scanning Electron Microscopy (SEM)

In order to evaluate the AgNPs in the sample, SEM (Buker/Germany) was utilized. On carbon-coated copper grids, thin films of the sample were created by dropping some of the filtrate on the grid, wiping away any extra solution using blotting paper, and letting the films dry for a whole night at room temperature under sterile circumstances. Using an EDX attachment on a scanning electron microscope, the silver nanoparticles were seen [22].

2.6. Antibacterial Activity

Using the disc diffusion method [18], the antibacterial activity of produced AgNPs was evaluated against a number of human diseases from both gram-negative and gram-positive bacteria that isolated from human diagnosis by VITC2 at Al- Sadr hospital in Misan, Iraq, as shown in Table (2). Each strain was uniformly swabbed into the distinct Muller Hinton agar plates using sterile cotton swabs.

Using a sterile micropipette, 10µg of produced AgNPs were poured over the plate. It was then applied and allowed to dry to a (6) mm sterile paper disc, so every disc contain10µg of biosynthesized AgNPs . Inhibitory zones developed all around the filter paper disc following a 24-hour incubation period at 37°C, demonstrating the bioactivity of the generated AgNPs. Using gentamicin (10 µg) as a reference, the clear zone diameters were measured and compared; triplicates were created.

Table (2). The collected Pathogenic bacteria from Al- Sadr hospital in Misan used in this study:

NO.	Pathogenic bacteria	Samples Source
1	*Staphylococcus aureus*	Ear
2	*Staphylococcus haemolyticus*	Wounds
3	*Staphylococcus hominis*	Nipple discharge
4	*Escherichia coli*	Urine
5	*Pseudomonas aeruginosa*	Burns
6	*Klebsiella pneumonia*	Urine
7	*Salmonella typhi*	Blood
8	*Enterobactor cloacae*	Wounds
9	*Staphylococcus lentus*	Urine
10	*Proteus mirabilis*	Wounds

2.7. Antitumor Activity

Breast cancer cells known as Mcf7 were acquired from the Basrah branch of the Iraq Biotech Cell Bank and grown in RPMI 1640 (Gibco, USA) with 10% fetal bovine serum, 100 units/mL penicillin, and 100 g/mL streptomycin. Cells were reseeded at 50% confluence, passaged twice weekly with Trypsin-EDTA, and incubated at 37°C with 5% CO2. In order to identify the cytotoxic effect, 96 well plates were used for the MTT cell viability assay. 1×10^{4} cells of the mcf7 cell line were placed in each well. After 24 hours or when a confluent monolayer was reached, cells were treated with the biosynthesized AgNPs at five concentration (10, 30, 60, 80, 100) µg/ml.

Following 72 hours of therapy, by removing the media, adding 28 liters of a 2 mg/ml MTT solution (Gibco/USA), and incubating the cells for 2 hours at 37 °C, cell viability assessed. The crystals in the wells were solubilized after the MTT solution was removed by adding 100ul of DMSO (Dimethyl Sulphoxide) and incubated at 37°C for 15 minutes while shaking.The assay was performed three times[18] and the absorbency was evaluated using a microplate reader at 620 nm (test wavelength).

3. Results and Discussion

The bacteria was cultured on culture media after the incubation period, and then it was purified on transfer media. The isolates were genotypically identified [19].

3.1. Genotypic Identification of the Isolated Strains

Genomic DNA was isolated using the previously described process and electrophoresed. Two bands with the same electrophoretic level are seen in the UV document that was generated, showing the presence of genomic DNA Figure (1). The 16sRNA gene was amplified using the universal 16sRNA gene primers given in table (1) utilizing the two DNA samples as templates for PCR. After that, the PCR product was electrophoresed on an Agarose gel and recorded on a gel document. The resulted 16sDNA bands were 1584 bp in size. Online NCBI blast software was used to compare each of the two resulting sequences, NCBI data base The first isolation A11 (the new one) It was registered for the first time in Iraq on GenBank because it was a new strain, so it was registered in my name in GenBank as *Microbacterium paraoxydans* strain shahooda, *16S rRNA* gene, Sequence ID: MZ701742.1, Length: 1388bp.. The *16SrRNA* sequencing from the second isolation A12 yielded 949 base pairs, found to be nearest to the sequence of *Microbacterium lacticum.* Strain STM54 *16S rRNA* gene partial sequence, length: 949 bp, 100%, Sequence ID: KY393059.1.

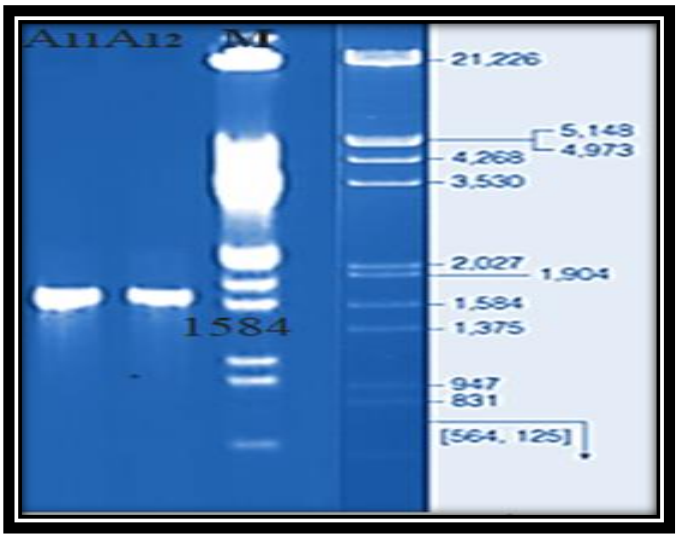

Figure (1). Genomic DNA extract from Bacterial Isolates that Electrophorese on 1 Percent Agarose Gel at 80volts, for 80min. Photograph Using a UV Gel Viewer, M:100bp DNA ladder.

3.2. Nanoparticles Formation

This study concentrated on the extracellular synthesis of silver nanoparticles by supernatant using *Microbacterium sp*. The first indication of silver nanoparticle formation was the color change from white to reddish brown after the incubation period, Figure (2).

This shows that the isolated bacteria had enzymatic reduction by electron shuttle mechanism supporting the reduction of metallic ions. Metal NPs are produced by NADH dependent nitrate reductases, which need cofactors such NADH as cofactors. Nitrate reductase, along with other components, including cofactors NADH and NADH-dependent enzymes, is released by B. licheniformis, which may be the cause of the bioreduction of Ag^{+} to Ag^{0} [26].

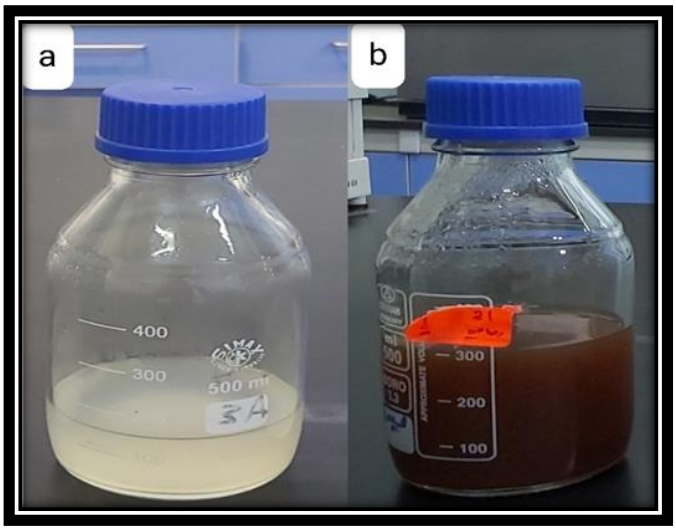

Figure (2). a- before synthesis. b- after formation of AgNPs.

3.3. Characterization of Ag Nanoparticles

3.3.1. UV-Vis spectroscopy

The intense color of the distributed silver nanoparticles was due to the absorption of the surface plasmon resonance spectrum (SPR) of silver nanoparticles. Metallic bio-nanoparticles, as a result, metallic bio-nanoparticles have a distinctive optical absorption spectrum in the UV visible region (300-800). The optical

absorption spectrum used in this study was at a wavelength of 489 nm. The spectra clearly showed a rise in silver solution intensity over time as the procedure went on, indicating the emergence of more silver nanoparticles in the solution. Figure (3) demonstrates that the reaction has reached equilibrium after 72 hours because there is no discernible variation in the UV-Vis spectra of the reaction product.

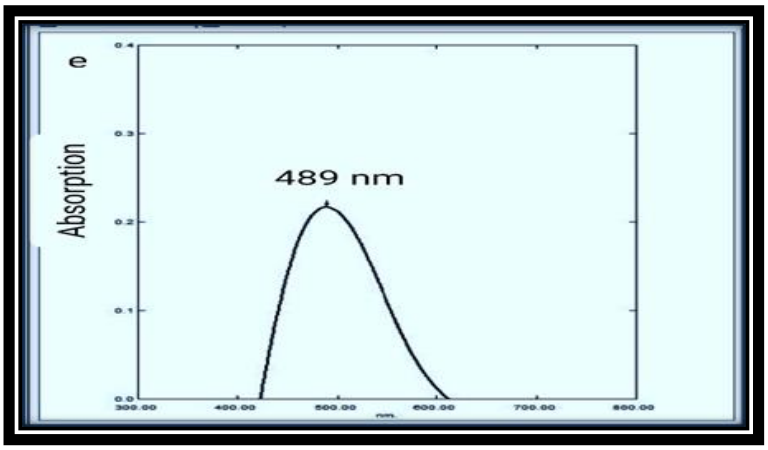

Figure (3). UV-Vis sp. synthesized by using *Microbacterium* sp. showed a peak at 489nm wave length.

3.3.2. XRD Analysis

Utilizing X-ray Diffraction, further research on silver nanoparticles was conducted. Figure (4) shows the crystal structure study and evaluation of the XRD phase of green-produced AgNPs. In the XRD examination, 2 theta = 28.3, 32.5, and 48.1 values were used to calculate the diffraction Standards (JCPDS) silver file No. (04–0783) for reflections (122), (111), and (200), respectively. AgNPs are FCC (face-centered and cubic) because they have an elemental (Ag^o) and are spherical and created crystalline.

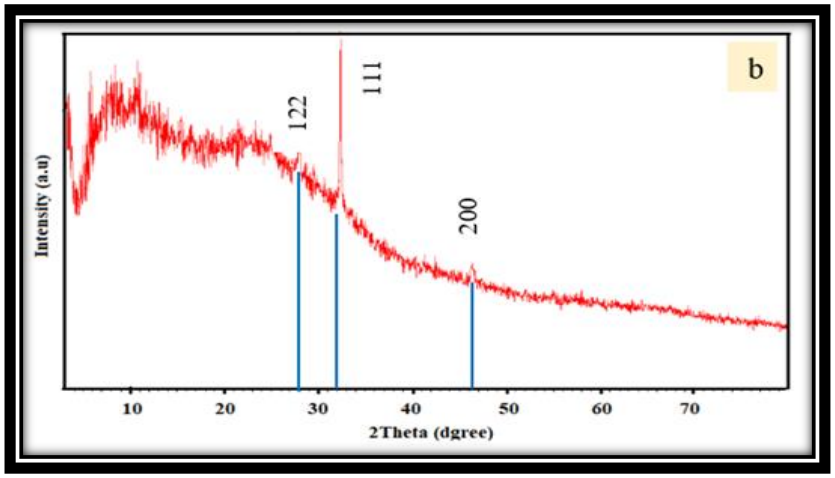

Figure (4). XRD of synthesized AgNPs analysis, Ag file No. (04– 0783).

3.3.3. TEM Analysis

The size and form of the particles were determined using TEM.As seen in this TEM image, Figure (5), silver particles with an measuring ruler of around 50 nm are evenly distributed and mostly spherical in shape.

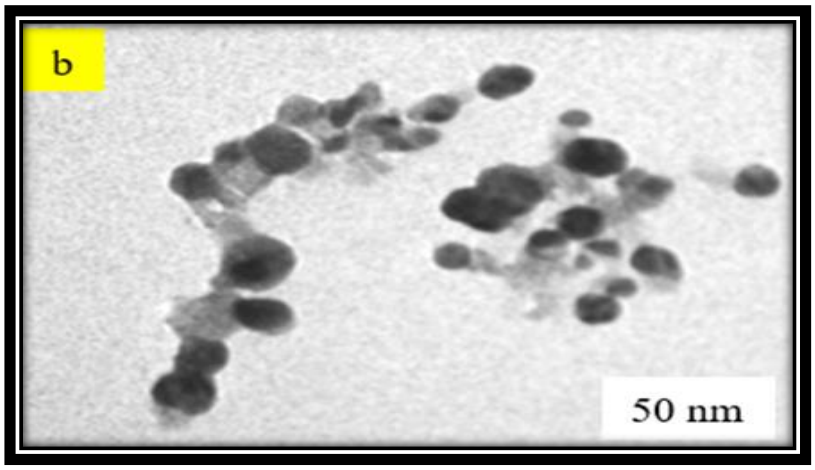

Figure (5). TEM image for silver nanoparticles

3.3.4. SEM Analysis

Silver nanoparticles made through biological synthesis were generally uniformly spherical Scanning Electron Microscopy analysis of biogenic AgNPs fabricated by the two strains showed homogenous, well-dispersed AgNPs, and the most predominant shape found to be spherical. Silver nanoparticles were produced as a result of the interactions of hydrogen bonds and electrostatic interactions between the bioorganic capping molecules attached to the AgNPs according to earlier research [20].

The absence of direct contact between the nanoparticles even inside the aggregates suggested that they were crystalline in structure and had been stabilized by a capping agent and the size was 41.55nm and 44.51nm, Figure (6).

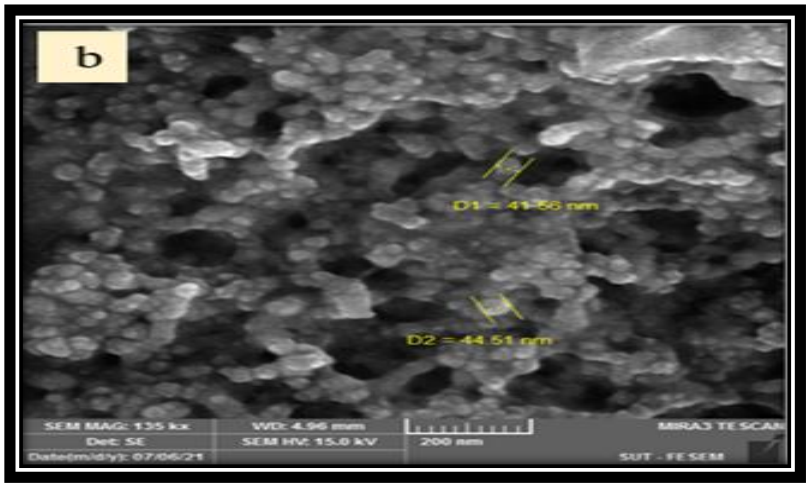

Figure (6). Scanning Electron Microscopy of AgNPs synthesize by *Microbacterium* sp.

3.4. Energy dispersive Spectroscopy X-ray (EDX)

The results show extremely high silver peaks, suggesting that molecules attached to the surface of the AgNPs may have had a role in the reduction of silver ions to elemental silver. The silver's thick peak was a blatant sign that silver nanoparticles had formed from Ag^{+}, Figure (7).

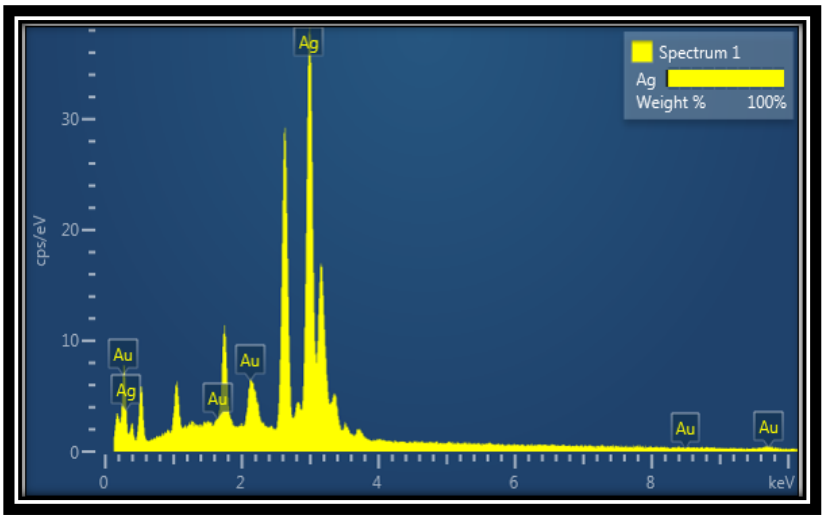

Figure (7). EDX for silver nanoparticles

3.5. Antimicrobial Activity

Nanoparticle was found to be efficient against bacterial infections in antimicrobial tests. Figure (9) show the comparison of both Gram-negative and Gram-positive bacteria with the antibiotic Gentamicin. The lowest inhibition zone was 6 mm on pseudomonas aeruginosa bacteria, as shown in Table (3). Silver nanoparticles produced by *Microbacterium lacticum* showed the largest inhibition zones (38mm) against ***Staphylococcus aureas*** bacteria, which was very large compared to antibiotics (Gentamicin) in this project. This largest inhibition zone of the synthesized AgNPs on pathogenic bacteria because nanoparticles affected on either the cell wall causes cell wall distraction or formation of reactive oxygen species (ROS), generation of reactive oxygen species (ROS) by the AgNPs has also been considered a primary mode of cytotoxic action of AgNPs observed a high level of ROS in cells treated with AgNPs .In these conditions, it makes sense to say that the amount of surface area available for contact determines how tightly the particles are bound to the bacterium. Smaller particles will have a greater bactericidal impact than larger particles because they have a higher surface area accessible for contact .In order to better understand the underlying mechanism of silver's antibacterial activity, a great deal of research has been done in this area[23]. The many mechanisms involved in the bactericidal effect of silver have long been known. Enzymes involved in crucial biological activities, such as ion transport and transmembrane energy production, bind silver atoms to their thiol groups. The thiol's oxygen and hydrogen atoms undergo oxidation processes that silver catalyzes, creating disulfide bonds and preventing bacterial growth. Cellular structure changes result from changes in their biologically essential components, which can induce malfunctions and ultimately cell death [24].

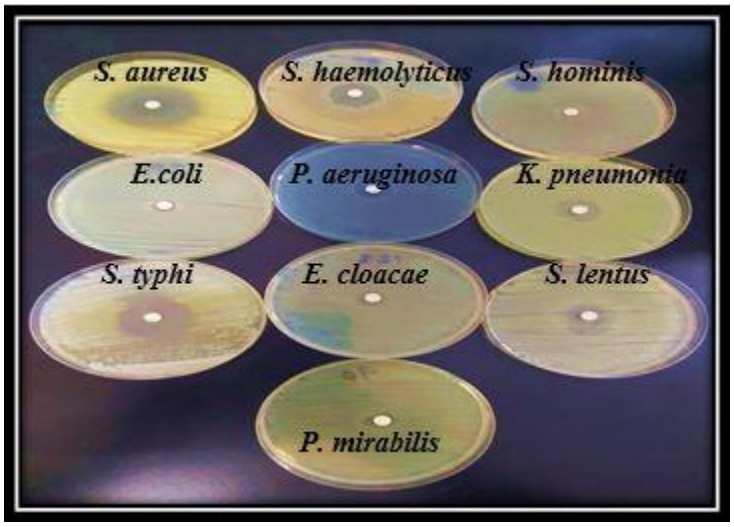

Figure (8). Antimicrobial activity against ten pathogenic bacteria.

Figure (9). Antimicrobial activity against the same pathogenic bacteria by antibiotic (Gentamicin).

Table (3). Inhibition zone by synthesized AgNPs and Gentamicin on ten specimen isolated from hospital.

Pathogenic bacteria	Inhibition zone of Gentamicin (antibacterial agent) (mm)	Inhibition zone (mm) of synthesized AgNPs
Staphylococcus aureus	9 mm	38 mm
Staphylococcus haemolytic	24.5 mm	22.5 mm
Staphylococcus hominis	7 mm	13 mm
Escherichia coli	14 mm	9.5 mm
Pseudomonas aeruginosa	13.5 mm	6 mm
Klebsiella pneumoniae	16.5 mm	18 mm
Salmonella typhi	24.5 mm	33.5 mm
Enterobacter cloacae	8 mm	12 mm
Staphylococcus lentus	28.5 mm	21 mm
Proteus merabilis	24.5 mm	10 mm

3.6. Antitumor Activity of AgNPs Biosynthesized Laboratory

AgNPs inhibited the MCF-7 cell line's ability to produce formazan at low doses, inhibiting it by roughly 81.32% at 100 µg/ml, and only 18.68% of the MCF-7 cell line were still alive (viable) after 72 hours of incubation. Figure (9) shows that the concentration of manufactured silver nanoparticles (10, 30, 60, 80, and 100 µg/ml) significantly altered the behavior of cancer cells, indicating that the toxicity of AgNPs increases as its concentration rises. The outcomes demonstrated that AgNPs significantly reduced the proliferation of MCF-7 cells, with an IC50 value of 24.93 µg/ml. This indicates that breast cancer cells are very sensitive to AgNPs, which have good anticancer efficacy. This outcome was consistent with what was stated by [20]. Through one of the appropriate pathways, they cause apoptosis. Such DNA cleavage is brought on by inhibition of topoisomerase I or II. In some cases, the inhibition of critical enzymes affects tumor-induced angiogenesis as well as signal transmission processes like proteases, mitochondrial permeabilization, and cellular metabolism [25].

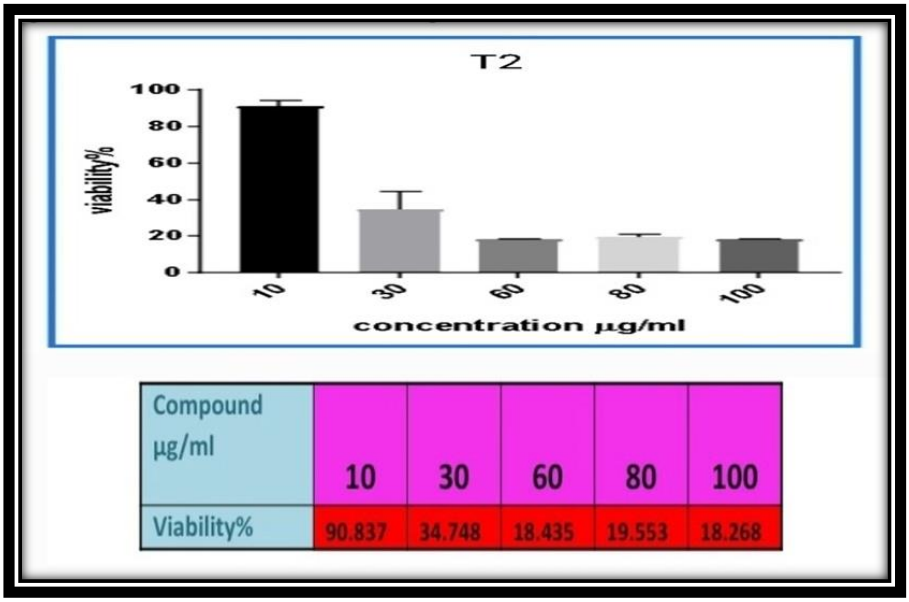

Figure (10). Viability in different concentrations of synthesized AgNPs (10, 30, 60, 80, 100) µg/ml on breast cancer cells line.

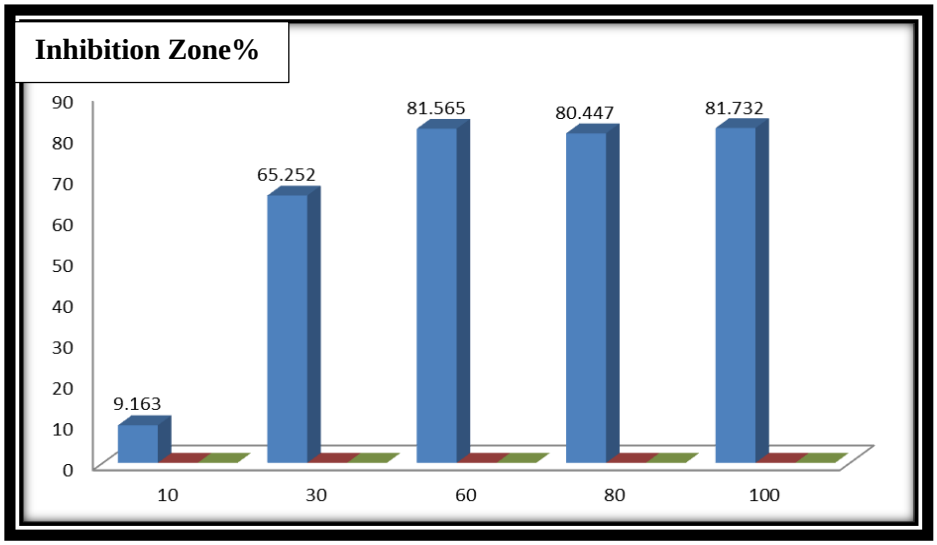

Figure (11). Inhibition Zone in different concentrations of synthesized AgNPs (10, 30, 60, 80, 100) µg/ml

on breast cancer cells line.

4. Conclusions

Novel strain was discovered (*M. paraoxydans* strain shahooda), from soil, extracellular synthesis of AgNPs has been employed effectively, characterization of AgNPs by physical test. Pathogenic bacteria can be inhibit by synthesized AgNPs, and also we can use AgNPs as anticancer on breast cancer cells.

Conflict of Interest: The authors declare that there are no conflicts of interest associated with this research project. We have no financial or personal relationships that could potentially bias our work or influence the interpretation of the results.

References

[1] Y. Tian, D. Hu, Y. Li, and L. Yang, "Development of therapeutic vaccines for the treatment of diseases," *Mol. Biomed.*, vol. 3, no. 1, pp. 1–30, 2022, doi: 10.1186/s43556-022-00098-9.

[2] M. Tariq, K. N. Mohammad, B. Ahmed, M. A. Siddiqui, and J. Lee, "Biological Synthesis of Silver Nanoparticles and Prospects in Plant Disease Management," *Molecules*, vol. 27, no. 15, 2022, doi: 10.3390/molecules27154754.

[3] J. A. Aboyewa, N. R. S. Sibuyi, M. Meyer, and O. O. Oguntibeju, "Green synthesis of metallic nanoparticles using some selected medicinal plants from southern africa and their biological applications," *Plants*, vol. 10, no. 9, 2021, doi: 10.3390/plants10091929.

[4] M. Sanjivkumar, R. Vaishnavi, M. Neelakannan, D. Kannan, T. Silambarasan, and G. Immanuel, "Investigation on characterization and biomedical properties of silver nanoparticles synthesized by an actinobacterium Streptomyces olivaceus (MSU3)," *Biocatal. Agric. Biotechnol.*, vol. 17, no. November 2018, pp. 151–159, 2019, doi: 10.1016/j.bcab.2018.11.014.

[5] N. H. M'sakni and T. Alsufyani, "Part B: Improvement of the Optical Properties of Cellulose Nanocrystals Reinforced Thermoplastic Starch Bio-Composite Films by Ex Situ Incorporation of Green Silver Nanoparticles from Chaetomorpha linum," *Polymers (Basel).*, vol. 15, no. 9, 2023, doi: 10.3390/polym15092148.

[6] Z. Kopecki, "Development of next-generation antimicrobial hydrogel dressing to combat burn wound infection," *Biosci. Rep.*, vol. 41, no. 2, pp. 1–5, 2021, doi: 10.1042/BSR20203404.

[7] S. Suneja, "Silver Nanoparticles: Revival of the Warrior in War against COVID-19," *Int. J. Res. Rev.*, vol. 7, no. 12, pp. 2454–2237, 2020, [Online]. Available: www.ijrrjournal.com.

[8] J. C. M. Espinosa, R. C. Cerritos, M. A. R. Morales, K. P. S. Guerrero, R. A. S. Contreras, and J. H. Macías, "Characterization of silver nanoparticles obtained by a green route and their evaluation in the bacterium of pseudomonas aeruginosa," *Crystals*, vol. 10, no. 5, pp. 1–13, 2020, doi: 10.3390/cryst10050395.

[9] F. M. M. Aldosari, "Characterization of Labeled Gold Nanoparticles for Surface-Enhanced Raman Scattering," *Molecules*, vol. 27, no. 3, 2022, doi: 10.3390/molecules27030892.

[10] T. M. Dewan and R. R. Hateet, "Detect the Antibacterial and Antitumor of synthesized Silver Nanoparticles Using Microbacterium sp," *Bionatura*, vol. 7, no. 2, 2022, doi: 10.21931/RB/2022.07.02.30.

[11] A. A. Hassan and A. F. Mahmoud, "Isolation, Phenotypic and Molecular Identification of Actinomycetes From Soil and Evaluation of Their Efficiency in Control of the Pathogen Botrytis cinerea Caused Gray Rot Disease on Eggplant," *IOP Conf. Ser. Earth Environ. Sci.*, vol. 1060, no. 1, pp. 0–16, 2022, doi: 10.1088/1755-1315/1060/1/012108.

[12] I. A. J. Ibrahim, T. A. Kareem, Y. M. Azeez, and H. K. Falhi, "Phylogenetic tree analysis based on the 16S sequence alignment for Klebsiella spp. Isolated from different sources," *Iraqi J. Sci.*, vol. 60, no. 12, pp. 2618–2628, 2019, doi: 10.24996/ijs.2019.60.12.10.

[13] P. B. Dayma, A. V Mangrola, S. P. Suriyaraj, P. Dudhagara, and K. Rajesh, "Synthesis of Bio-Silver Nanoparticles Using Desert Streptomyces Intermedius and Its Antimicrobial Activity Isolated," *J. Pharm. Chem. Biol. Sci.*, vol. 7, no. August, pp. 94–101, 2019.

[14] M. M. El-Adawy *et al.*, "Green synthesis and physical properties of Gum Arabic-silver nanoparticles and its antibacterial efficacy against fish bacterial pathogens," *Aquac. Res.*, vol. 52, no. 3, pp. 1247–1254, 2021, doi: 10.1111/are.14983.

[15] M. A. Khalil *et al.*, "Biosynthesis of Silver Nanoparticles by Marine Actinobacterium Nocardiopsis dassonvillei and Exploring Their Therapeutic Potentials," *Front. Microbiol.*, vol. 12, no. February, 2022, doi: 10.3389/fmicb.2021.705673.

[16] S. P. P., "Structural and Electrical Studies on Zinc Added Magnesium Oxide Nanoparticles," *J. Phys. Sci.*, vol. 31, no. 3, pp. 73–86, 2020, doi: 10.21315/jps2020.31.3.6.
[17] J. Zhu, S. Liu, O. Palchik, Y. Koltypin, and A. Gedanken, "Shape-controlled synthesis of silver nanoparticles by pulse sonoelectrochemical methods," *Langmuir*, vol. 16, no. 16, pp. 6396–6399, 2000, doi: 10.1021/la991507u.
[18] T. D. Tavares *et al.*, "Activity of specialized biomolecules against gram-positive and gram-negative bacteria," *Antibiotics*, vol. 9, no. 6, pp. 1–16, 2020, doi: 10.3390/antibiotics9060314.
[19] S. A. Bhatti *et al.*, "Evaluation of the antimicrobial effects of Capsicum, Nigella sativa, Musa paradisiaca L., and Citrus limetta: A review," *Front. Sustain. Food Syst.*, vol. 6, 2022, doi: 10.3389/fsufs.2022.1043823.
[20] S. Gurunathan, "Rapid biological synthesis of silver nanoparticles and their enhanced antibacterial effects against Escherichia fergusonii and Streptococcus mutans," *Arab. J. Chem.*, vol. 12, no. 2, pp. 168–180, 2019, doi: 10.1016/j.arabjc.2014.11.014.
[21] T. Miyoshi, T. Iwatsuki, and T. Naganuma, "Phylogenetic characterization of 16S rRNA gene clones from deep-groundwater microorganisms that pass through 0.2-micrometer-pore-size filters," *Appl. Environ. Microbiol.*, vol. 71, no. 2, pp. 1084–1088, 2005, doi: 10.1128/AEM.71.2.1084-1088.2005.
[22] V. Kathiravan, S. Ravi, S. Ashokkumar, S. Velmurugan, K. Elumalai, and C. P. Khatiwada, "Green synthesis of silver nanoparticles using Croton sparsiflorus morong leaf extract and their antibacterial and antifungal activities," *Spectrochim. Acta - Part A Mol. Biomol. Spectrosc.*, vol. 139, no. November 2018, pp. 200–205, 2015, doi: 10.1016/j.saa.2014.12.022.
[23] U. M, R. T, B. T, and R. R, "Antimicrobial Activity of Silver Nanoparticles Prepared Under an Ultrasonic Field," Int. J. Pharm. Sci. Nanotechnol., vol. 4, no. 3, pp. 1491–1496, 2011, doi: 10.37285/ijpsn.2011.4.3.8.
[24] G. Nam, S. Rangasamy, B. Purushothaman, and J. M. Song, "The application of bactericidal silver nanoparticles in wound treatment," Nanomater. Nanotechnol., vol. 5, no. 1, 2015, doi: 10.5772/60918.
[25] P. Shi et al., "Active targeting schemes for nano-drug delivery systems in osteosarcoma therapeutics," J. Nanobiotechnology, vol. 21, no. 1, pp. 1–27, 2023, doi: 10.1186/s12951-023-01826-1.
[26] J. Ali, N. Ali, L. Wang, H. Waseem, and G. Pan, "Revisiting the mechanistic pathways for bacterial mediated synthesis of noble metal nanoparticles," *J. Microbiol. Methods*, vol. 159, pp. 18–25, 2019, doi: 10.1016/j.mimet.2019.02.010.